JTTEE5 12:572-575

Corrosion Behavior of HVOF Coated Sheets

B.S. Yilbas, M. Khalid, and B.J. Abdul-Aleem

(Submitted 15 January 2002; in revised form 9 April 2002)

High velocity oxygen-fuel (HVOF) thermal spray coating finds application in industry due to its superior resistance to corrosion and thermal loading. In the HVOF process, the metallic powders at elevated temperature are sprayed at supersonic speed onto a substrate material. The powder granules sprayed impact onto each other, forming a mechanical bonding across the coating layer. In most of the cases, the distances among the particles (powder granules sprayed) are not the same, which in turn results in inhomogeneous structure across the coating layer. Moreover, the rate of oxidation of the powder granules during the spraying process varies. Consequently, the electrochemical response of the coating layer surfaces next to the base material and free to atmosphere differs. In the current study, the electrochemical response of a coating sheet formed during HVOF thermal spraying was investigated. NiCrMoNb alloy (similar to Inconel 625) wass used for the powder granules. Thermal spraying was carried out onto a smooth surface of stainless steel workpiece (without grid blasting), and later the coating layer was removed from the surface to obtain the coating sheet for the electrochemical tests. It was found that the corrosion rate of the smooth surface (surface next to the stainless steel surface before its removal) is considerably larger than that corresponding to the rough surface (free surface) of the coating sheet, and no specific patterns were observed for the pit sites.

Keywords: HVOF coating corrosion properties

1. Introduction

A thermal spray coating is widely used to protect the metallic surfaces from high temperature and harsh corrosion environments. One of the recent thermal spraying processes is the high velocity oxygen-fuel (HVOF) spraying. Although many parametric studies were performed on process-controlling parameters and coating quality, understanding of the physical and chemical processes involved needs to be explored further.

HVOF thermal spraying uses a gun, which utilizes an internal combustion process to generate supersonic gas velocities. The combustion fuel is mixed with oxygen in the gun. The powders of coating material are ejected directly into the combustion region of the gun. The semi-molten powder particles are accelerated with a high velocity combusted gas stream and impact onto the surface of the substrate material subjected to the coating. The standoff distance between the gun and the substrate surface is about 0.12-0.35 m. The surface of the substrate material is grid blasted prior to the thermal spraying, since it is essential to secure a sound bounding across the coating interface. The surface should be chemically cleaned from any kind of depositions prior to coating, and the temperature of the surface is usually kept between 150 and 175 °C during the thermal spraying process.

Considerable research studies were carried out to explore HVOF thermal spray process. Oxidation of stainless steel in high velocity oxyfuel process was investigated by Dobler et al.[1] They indicated that heat treatment of the surface after coating process reduced hardness, metallurgically enhanced bond strength, and enabled the spheroidization of oxide layers surrounding unmelted particles. Moreover, they showed that maintaining a relatively low particle temperature throughout the spraying process minimized oxygen pick-up by preventing an autocatalytic oxidation process and particle fragmentation upon impact. Salt fog corrosion behavior of HVOF thermal spray coatings was studied by Natishan et al.[2] They observed that for WC/Co coatings, no pitting or blistering occurred on the faces, but a significant amount of pitting occurred along the edges. The durability of thermal sprayed cerment coatings for application in aqueous environments with or without the influence of erosion was investigated by Neville and Hodgkiess.[3] They showed that the corrosion behavior in aqueous environments requires careful consideration when selecting a coating material. The electrochemical methods for characterization of thermal spray corrosion resistant stainless steel coatings were investigated by Hofman et al.[4] They showed that the electrochemical response of the arc spray coatings studied was independent of substrate type; i.e., the underlying alloy did not contribute to the corrosion process and only the coating itself was attacked. The severe fluid erosion and corrosion of drill bits using thermal spray coatings were investigated by Kembaiyan and Keshavan.[5] They showed that the detonation gun coated tungsten carbide coatings exhibited superior erosion resistance than all other coatings tested.

In light of the above arguments, in the current study, the electrochemical response of HVOF thermal sprayed coating sheet was carried out. The powder identical to Inconel 625 alloy properties was sprayed on to the steel surface without grid blasting. The coating as, then, removed (pealed off) from the steel base and prepared for electrochemical tests. Potentiodynamic tests was conducted, and TAFEL results are presented here. Scanning electron microscopy (SEM) was carried out to investigate the surface morphology before and after the electrochemical tests.

B.S. Yilbas and **B.J. Abdul-Aleem,** Mechanical Engineering Department, KFUPM, Dhahran, Saudi Arabia; and **M. Khalid,** Chemistry Department, KFUPM, Dhahran, Saudi Arabia. Contact e-mail: bsyilbas@kfupm.edu.sa.

Table 1 Composition of Powder Used During Thermal Spraying

Powder	Composition, wt.%
Ni	Balance
Cr	21.5
Mo	9
Nb	3.7

Table 2 Process Parameters of Thermal Spray

Parameter	Value
Oxygen, Pressure, kPa	1034
Fuel Pressure, kPa	620
Air Pressure, kPa	724
Powder Feed Rate, m^3/h	0.81
Spray Rate, kg/h	6.35
Spray Distance, m	0.28

2. Experimental

The hybrid HVOF system was used to obtain the coating sheet. Propane was used in the combustor, and powder flow was centered by using axial powder feeding with auxiliary air, which surrounded the particle stream during the spraying. The powder unit was based on the fludized bed system, which could include closed loop control. The control unit provided precision of operation.

Nickel-based powder (NiCrMoNb equivalent to Inconel 625) was used and the powder had the size 35-55 μm with spherical shape. It had excellent high-temperature oxidation and corrosion properties. The chemical composition of the powder is given in Table 1.

To obtain a coating sheet, stainless steel surface with low surface roughness (without grid blasting) was used as a base substrate material. The powder was sprayed onto the base material initially, and later the coating was removed (pealed off) from the stainless steel surface. Moreover, thermal spraying resulted the coating thickness in the order of 400 μm. The coating sheet was cut into 30 × 20 mm^2 (length × height) size for electrochemical tests. The process parameters for thermal spraying are given in Table 2.

The electrochemical tests was conducted in 0.1N H_2SO_4 + 0.05N NaCl using an EG&G PARC model 273 A Potentiostat-Galvanostat (New Jersey, USA). The workpieces were degreased in benzene and washed with de-ionized water prior to the electrochemical tests. The electrochemical cell was a three-electrode cell. An Ag/AgCl electrode was used as a reference electrode. The working electrode was the specimen under test. A platinum electrode of 1 cm^2 was used as an auxiliary electrode. TAFEL polarization experiments were conducted to determine the corrosion rates.

SEM microscopy of the surfaces before and after the electrochemical tests was conducted using JEOL JDX-3530 (Tokyo, Japan).

3. Discussion

The electrochemical response of HVOF thermal sprayed coating sheet was investigated. The coating sheet is obtained through coating of stainless steel surface with the powder equivalent to Inconel 625 and then the coating layer is removed from the surface of the stainless steel base material. Since both surfaces of the coating sheet have different metallurgical and chemical characteristics, the electrochemical tests are conducted for both surfaces of the coating sheet. To examine the pit sides, SEM microphotography is carried out.

Figure 1 shows the rough and smooth surfaces of HVOF coating sheet. The size of powder granules in the smooth surface region is low due to the fractured granules after impacting the stainless steel surface. The patterns of surface roughness of the base material are evident, i.e., surface roughness of the base material is low. In the case of rough surface, locally scattered small voids can be observed. However, the depth of the voids is limited to the size of the powder granules. When examining the cross section of the coating sheet, neither a pinhole nor microvoid are observed across the coating sheet.

Figure 2 shows TAFEL polarization curves of Inconel 625 alloy, the rough and smooth surfaces of coating sheet. From Table 3, it is noted that the smooth surface of the coating sheet (surface next to the stainless steel workpiece during HVOF coating) has the lowest corrosion potential of −0.316 V as compared with −0.257 V for the rough surface (front surface of the coating sheet). The corrosion rate of the rough surface was found to be 0.200 mmpy compared with 115 mmpy for the smooth surface. This is an enhancement in corrosion protection by a factor of 60. Both the rough and smooth surfaces show the corrosion potential less than that for Inconel 625 (−0.152 V). From Fig. 2, the general performance of the rough surface resembles the Inconel 625 workpiece. A protection current is observed at the end of the TAFEL polarization curves indicating the formation of oxide product, which leads to the decrease in corrosion current for both Inconel 625 and the rough surface of the coating sheet. Moreover, it is possible that during the spraying process, the powder granules impacting with high speed onto the stainless steel surface could fracture. This, in turn, results in relatively smooth surface of the coating sheet next to the stainless steel surface. The resulting surface may increase the anodic dissolution in the surface region; i.e., small particle spacing in the surface region of the coating sheet accelerates the removal of the metal ions via complex ion formation.

Figure 3 and 4 show SEM micrographs of pit sites corresponding to front (rough surface) and back surfaces (smooth surface) of the coating sheet. It should be noted that the smooth surface represents the surface, which was initially in contact with stainless steel workpiece before its removal. It can be observed that no specific pattern of the pit geometry occurs for both surfaces, provided that the pit size is relatively larger at the smooth surface than that corresponding to the rough surface. This occurs due to: (a) partially fractured powder granules, which are small in size, gives rise to less particle spacing at the smooth surface, which in turn influences the homogeneous structure of the surface, and (b) the particles oxided at the rough surface enhances the corrosion resistance of the surface. Moreover, pit geometry shows significant lateral growth along the surface leading to expanded pits. The pit growth saturates after some time, which indicates the reactivation of pits being passivated. In this case, the secondary micropits play important role in the reactivation process. This is particularly true for the

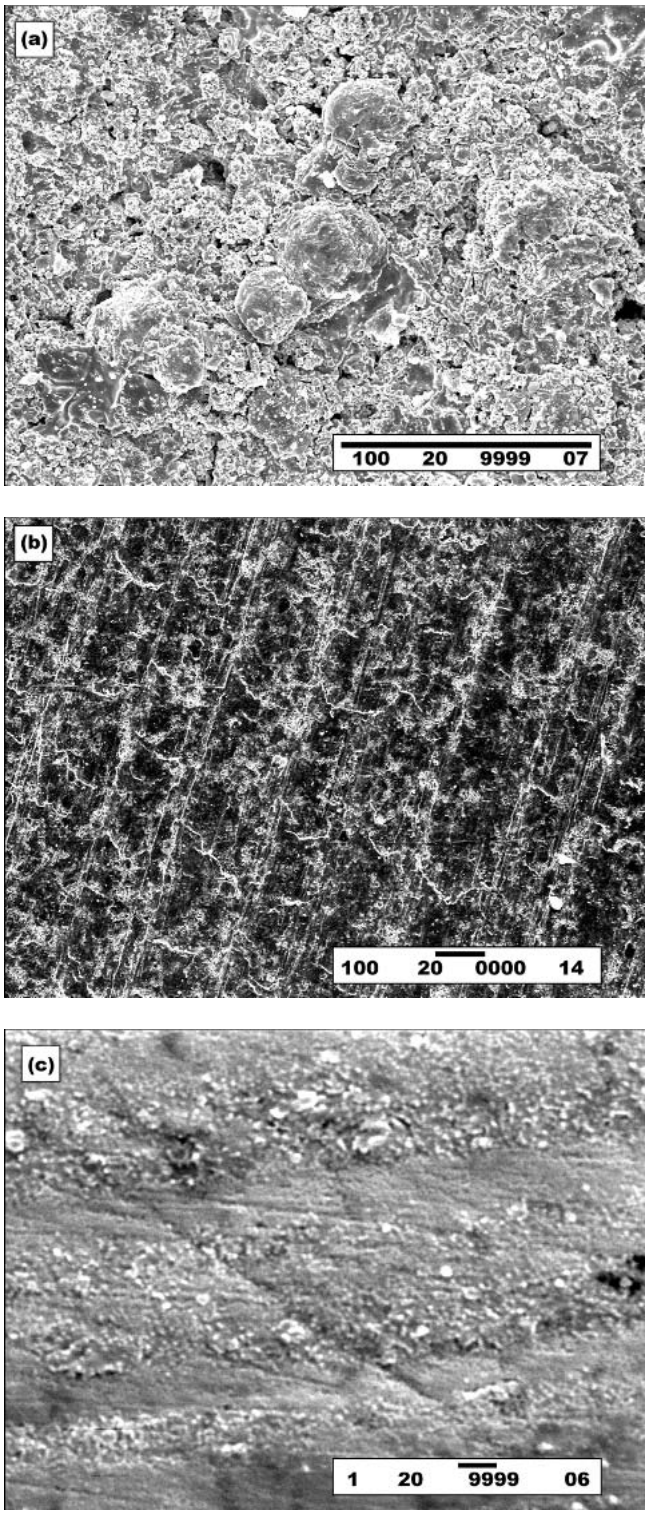

Fig. 1 SEM micrographs of rough and smooth surfaces of a coating sheet

smooth surface of the coating sheet. In addition, severe pitting over the powder boundaries is evident, and the formation of oxide species is likely in the surface region. During the pit growth, the pit base acts as an anode galvanically coupled to the external cathodic area leading to a steeper potential gradient in the pit;

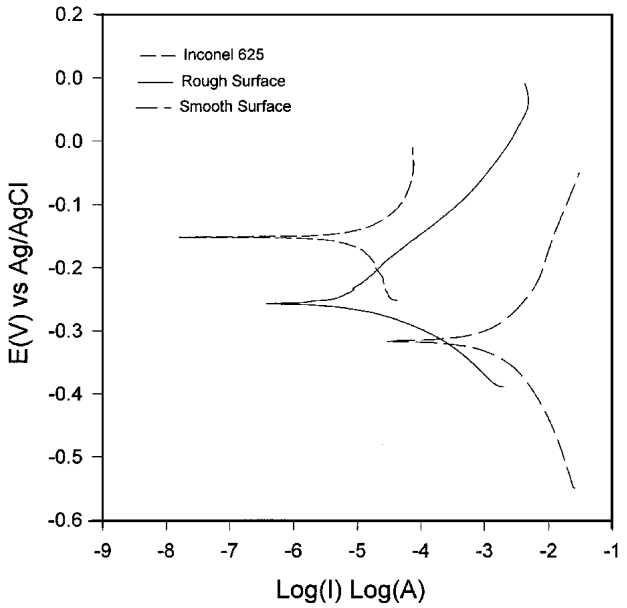

Fig. 2 Tafel plot of Inconel 625, rough and smooth surfaces of coating sheet in 0.1N H_2SO_4 and 0.05M NaCl, at scan rate of 0.166 mV/s

i.e., the pit depth increases locally at the pit base. However, formation of insoluble pit corrosion product increases the ohmic resistance to current flow inside the pit; this, in turn, causes polarization to a more noble potential and a lower corrosion current.

4. Conclusions

The electrochemical response of HVOF sprayed NiCrMoNb powder coating sheet is investigated. The thermal spraying is achieved onto stainless steel workpiece with smooth surface and the coating is later removed from the steel surface. The coating sheet is cut and prepared for the electrochemical tests in aqueous electrolytic solution of 0.1N H_2SO_4 + 0.05M NaCl. It is found that the corrosion rate is considerably higher at the smooth surface of the coating sheet as compared that corresponding to the rough surface. The specific conclusions derived from the current study can be listed as follows:

- Locally scattered voids are observed at the rough surface of the coating sheet, provided that the depth of the voids is limited to powder granules size. Moreover, neither voids nor pinhole are observed across the coating sheet.
- The corrosion resistance of the rough surface is similar to that corresponding to Inconel 625 alloy. On the other hand, the corrosion rate increases substantially for the smooth surface of the coating sheet. This is due to (a) oxidation of powder granules in the region of the smooth surface is highly unlikely, which in turn lowers the corrosion resistance, and (b) the powder granules impacting onto a stainless steel surface could fracture giving rise to non-homogenous microstructure at the surface.
- The elongated pits at the surface are observed. The pit site is shallow and the passive corrosion products in the pit site suppress the reactivation of the pit sites.

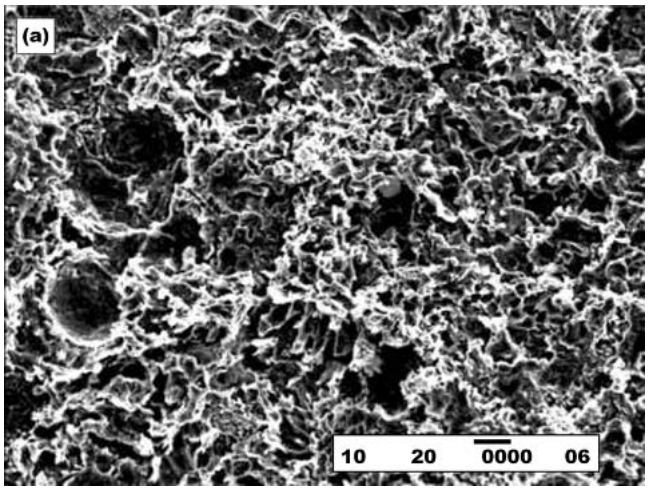

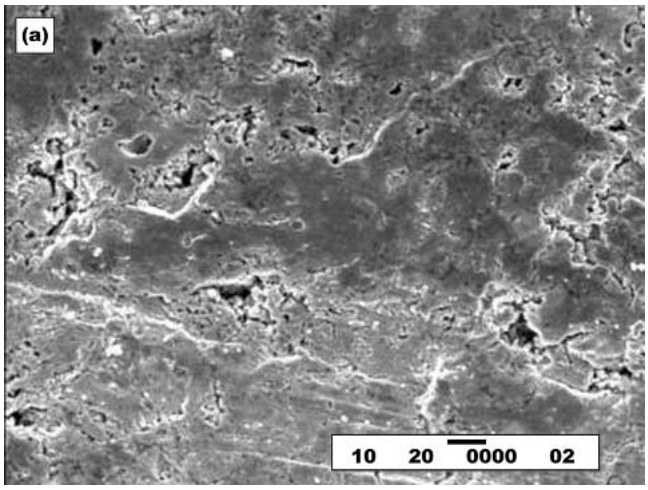

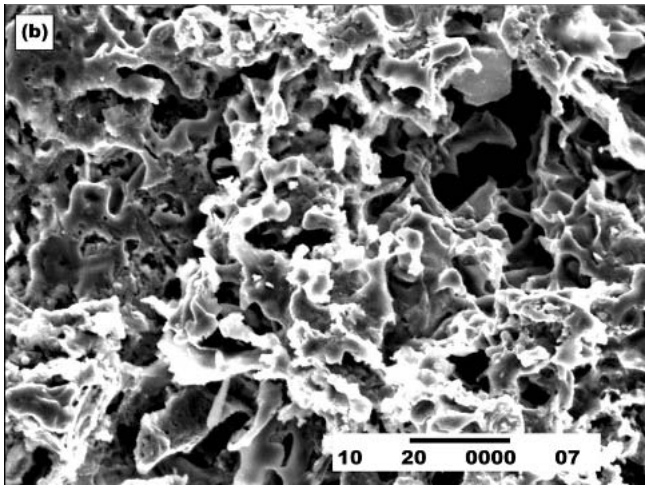

Fig. 3 SEM micrographs of pit sites at the rough surface of the coating sheet

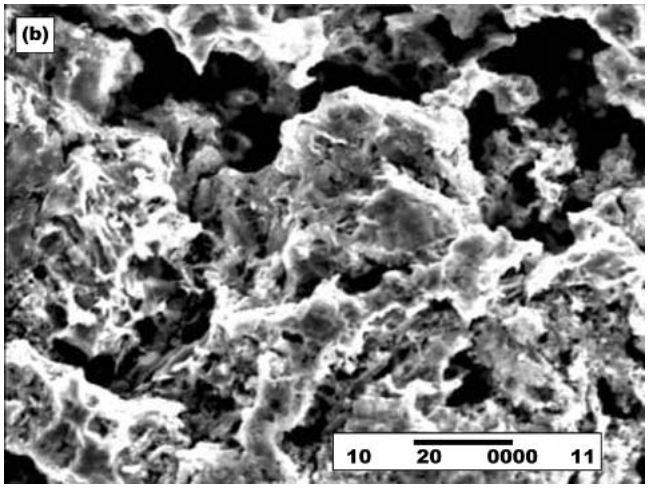

Fig. 4 SEM micrographs of pit sites at the smooth surface of coating sheet

Table 3 Corrosion Parameters for Inconel 625, the Rough and Smooth Surfaces of Coating Sheet

	E (I = 0), mV	Cathodic TAFEL, V	Anodic TAFEL, V	Corrosion Current, mA/cm^2	Corrosion Rate, mm/y
Inconel 625	−0.152	2.00	0.122	31.7×10^{-3}	0.770
Rough Surface	−0.257	0.100	0.05	7.6×10^{-3}	0.200
Smooth Surface	−0.316	0.340	0.300	4.40	115

Acknowledgments

Acknowledgements are due to King Fahd University of Petroleum and Minerals.

References

1. K. Dobler, H. Kreye, and R. Schwetzke: "Oxidation of Stainless Steel in the High Velocity Oxy-Fuel Process," *J. Therm. Spray Technol.,* 2000, *9,* pp. 407-13.
2. P.M. Natishan, S.H. Lawrence, R.L. Foster, J. Lewis, and B.D. Sartwell: "Salt Fog Corrosion Behavior of High-Velocity Oxygen-Fuel Thermal Spray Coatings Compared to Electrodeposited Hard Chromium," *Surf. Coat. Technol,.* 2000, *130,* pp. 214-23.
3. A. Neville and T. Hodgkiess: "Corrosion Behavior and Microstructure of Two Thermal Spray Coatings," *Surf Eng.,* 1996, *12,* pp. 303-12.
4. R. Hofman, M.P.W. Vreijling, G.M. Ferrari, and J.H.W. Wit: "Electrochemical Methods for Characterization of Thermal Spray Corrosion Resistant Stainless Steel Coatings," *Mater. Sci. Forum,* 1998, *289-292,* pp. 641-54.
5. K.T. Kembaiyan and K. Keshavan: "Combating Severe Fluid Erosion and Corrosion of Drill Bits Using Thermal Spray Coatings," *Wear,* 1995, *186-187,* pp. 487-92.